

## Multiparametric MRI to Differentiate High-Risk From Low-Risk Prostate Cancer

Olga Starobinets<sup>1</sup>, Jeffry Simko<sup>2,3</sup>, Kyle Kuchinsky<sup>2</sup>, John Kornak<sup>4</sup>, John Kurhanewicz<sup>1,5</sup>, Dan Vigneron<sup>1,5</sup>, Peter Carroll<sup>3</sup>, Kirsten Greene<sup>3</sup>, and Susan Noworolski<sup>1,5</sup>  
<sup>1</sup>Graduate Group in Bioengineering, University of California, San Francisco and Berkeley, San Francisco, CA, United States, <sup>2</sup>Pathology, University of California, San Francisco, CA, United States, <sup>3</sup>Urology, University of California, San Francisco, CA, United States, <sup>4</sup>Epidemiology and Biostatistics, University of California, San Francisco, CA, United States, <sup>5</sup>Radiology and Biomedical Imaging, University of California, San Francisco, CA, United States

**Purpose:** In the current era of promoting active surveillance for men with low-risk prostate cancer, it is critically important to be able to distinguish the high-risk prostate cancers from the low-risk. Current methods of determining the aggressiveness of prostate cancer is limited to Gleason Score grading of tissue samples obtained during a transrectal ultrasound (TRUS) guided prostate biopsy, a painful procedure, prone to sampling errors. A TRUS biopsy can miss a clinically significant cancer up to 30% of the time<sup>1</sup>. Multiparametric (MP) MR allows for a noninvasive evaluation of the prostate cancer. While MP MR has been well established for identifying prostate cancer<sup>2,3</sup>, its role has not been well evaluated for discriminating the high-risk from the low-risk cancers, in part due to challenges arising from the heterogeneity of the disease (requiring detailed histopathology) and the need for sophisticated modeling. The purpose of this study was to use a combination of semi-quantitative and pharmacokinetically modeled parameters derived from dynamic contrast-enhanced (DCE) MRI, diffusion MR and MRI to differentiate high-risk from low-risk cancers, using step-section histopathology, complete with a percentage breakdown of Gleason grades and benign tissues, as a reference standard.

**Methods:** Thirty-nine men with untreated prostate cancer received 3T MR scans prior to undergoing prostatectomy. DCE MRI was performed using a 3D FSPGR sequence with TR/TE/flip=5/2.1ms/6°, 2.7mm slices, and a single-dose of Gd-DPTA over ~5 minutes. Post prostatectomy, prostate specimens were processed whole-mount. During histological review, cancerous regions were outlined and graded, and the percentage of cancer estimated by the same prostate pathologist. ROIs were manually drawn on T2-weighted images based on the digitized histopathology slides, following a consensus of two readers, keeping within homogeneous regions. A total of 216 cancer ROIs were drawn. Only ROIs containing more than 50% cancer were included in the analysis. In the peripheral zone Gleason Score (GS) 6 (n=27 regions were outlined in N=13 patients), GS7 (n=60, N=17), GS8 (n=25, N=11), and noncancerous cystic atrophy regions (n=117, N=33) were identified.

MR apparent diffusion coefficient (ADC), fractional anisotropy (FA), coil-corrected<sup>4</sup>, T2-weighted image intensity, and DCE MRI parameters: time to peak, maximal enhancement slope, peak enhancement, and washout slope were calculated. Pharmacokinetically modeled parameters were determined from fits to an extended Tofts-Kermode ( $K^{trans}$ ,  $V_{ees}$ )<sup>5</sup> and to a Luminal water model ( $K^{trans}$ ,  $V_{ees}$ ,  $V_L$ ), which assumes Gd-DTPA cannot reach the luminal space,  $V_L$ <sup>6</sup>. Within each individual, ROIs were grouped in accordance to tissue type and a weighted average based on ROI areas was calculated for each metric of interest. Due to low numbers, central gland cancer regions were grouped together. Peripheral zone cancers were grouped into high-risk (G4+3 and higher) and low-risk (G3+3 and G3+4) and compared between groups and to cystic atrophy.

**Results:** In the central gland, cancer was lower on ADC ( $p<0.001$ ) and higher on FA ( $p<0.03$ ) and on enhancement slope ( $p<0.03$ ) than cystic atrophy. In the peripheral zone, significant differences among groups were observed (Figure 1).

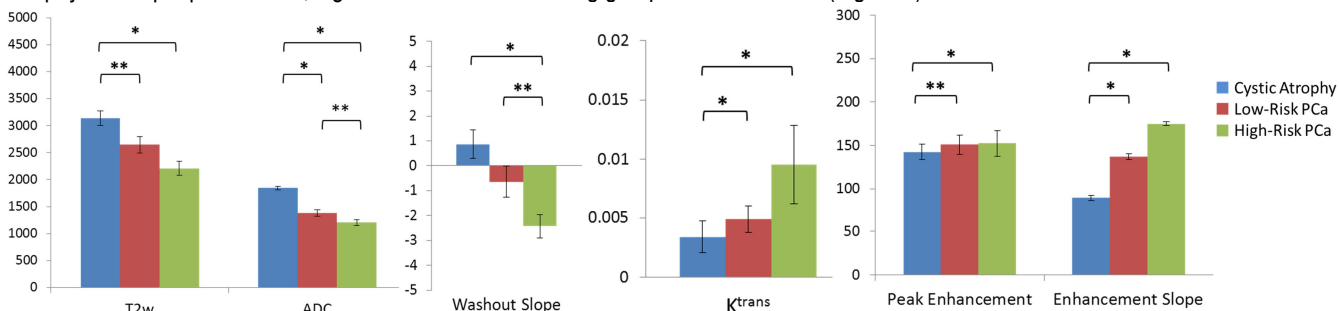


Figure 1: Average Peripheral Zone Measures: T2w intensity (AU), ADC ( $\times 10^{-3} \text{mm}^2/\text{sec}$ ), washout slope (%baseline/min),  $K^{trans}$  (1/min), peak enhancement (%baseline), enhancement slope (%baseline/min) in cystic atrophy, low and high-risk prostate cancer. Error bars reflect standard error of the mean, \* $p<0.01$ , \*\* $p<0.05$ .

High-risk cancers had significantly lower ADC and washout slope than low-risk cancers ( $p<0.05$ ). A stepwise, logistic regression yielded significant parameters of T2w intensity, ADC, enhancement slope, washout slope, and Luminal  $K^{trans}$  with a combined model AUC of 0.95 for detecting high- versus low-risk cancers. Without ADC, logistic regression combining Luminal  $V_{ees}$ , T2w intensity and washout slope yielded an AUC of 0.87 for discriminating high- versus low-risk prostate cancer.

**Discussion:** In this study diffusion and DCE MRI measures showed significance in discriminating high-risk from low-risk peripheral zone prostate cancers, with their combination yielding excellent discrimination (ROC AUC=0.95). In the absence of ADC (seen for patients with hip replacements), by combining T2w intensity and DCE parameters, a very good discrimination of high-risk from low-risk cancer was still observed (AUC=0.87), underlining the ability of a MP MR exam to provide an excellent and robust characterization of prostate tissues. An accurate, noninvasive evaluation of prostate cancer aggressiveness can prompt patients with indolent prostate tumors to pursue active surveillance (avoid unnecessary treatment) and motivate patients with aggressive disease to pursue critically important definitive treatment of their cancer.

**References:** 1-Taira et al. Prostate Cancer and Prostatic Dis. 2010. 2-Isebaert et al. JMRI 37(6):1392-401. 3-Rais-Bahrami et al. J Urology 2013; 190(5):1721-7. 4-Noworolski et al. JMRI 2010; 32(3): 652-62. 5-Tofts JMRI 1997;91-101. 6-Noworolski et al. ISMRM (2011).